



Hot cracking in duplex stainless steel weldments — a review

Elin M. Westin¹

Received: 18 February 2022 / Accepted: 27 April 2022 / Published online: 6 May 2022
© International Institute of Welding 2022, corrected publication 2022

Abstract

Due to primary ferritic solidification, the duplex stainless steels are generally considered resistant to solidification cracking. Although very few publications are available on any form of hot cracking of duplex grades, these alloys are not immune to the phenomenon. This review paper gives an introduction to solidification cracking in stainless steel welds, the weldability of the duplex grades, and possible circumstances where solidification cracking may occur. As the duplex alloys are increasingly used in applications where heavy-wall material is welded under highly restrained conditions, the risk for hot cracking also increases. Ways to detect and inspect cracks are discussed. Particular focus is placed on the flux-cored arc welding (FCAW) process where high welding speeds can be reached and especially when using ceramic backing for the root pass. Different compositions and slag concepts by various manufactures for different wires are debated as these can have a considerable effect on the susceptibility.

Keywords Duplex stainless steel · Welding · FCAW · Solidification cracking

1 Welding of duplex stainless steels

Ferritic-austenitic (duplex) stainless steels consist of a ferritic matrix contributing high strength and resistance to stress corrosion cracking (SCC), and islands of austenite increasing the ductility and resistance to local corrosion as compared to ferritic alloys. Thanks to the combined advantages, typical applications range from domestic water heaters to construction of bridges and storage tanks for chemicals. Some of the most common duplex grades are listed in Table 1.

To optimize the material performance, the fraction of ferrite and austenite should approximately be equal. In the base material, this is reached by controlled thermo-mechanical rolling and heat treatment. When welding duplex alloys, however, the final austenite distribution is a complex function of the chemical composition and thermal cycle(s). This is influenced by the composition of the base material, filler metal and shielding gas together with arc energy, dilution

from base material and previous passes, and the total number of passes. The solidification is fully ferritic and diffusion-controlled transformation to austenite occurs in the solid state during subsequent cooling [1–3]. The existing base metal grains at the fusion line act as the substrate for nucleation [4]. The temperature range between the solidus and austenite formation is determined by the chemical composition and greatly affected by the nitrogen and nickel contents. For this reason, modern duplex stainless steels are alloyed with nitrogen to promote austenite formation in the weldment and it is recommended to use filler metals over-alloyed in nickel [5]. There exist different solid wires for the processes gas tungsten arc welding (GTAW), gas metal arc welding (GMAW) and submerged arc welding (SAW), flux-cored wires for flux-core arc welding (FCAW) and covered electrodes for shielded metal arc welding (SMAW). Table 2 presents examples of standardized consumables used for welding of duplex stainless steels.

A highly ferritic weld may have decreased resistance to pitting [6–9] and hydrogen cracking [10–12], whereas an excessively austenitic weld could have lower resistance to SCC [13, 14]. The formation of austenite is also dependent on the cooling time and the amount increases at lower cooling rates [15, 16].

In multipass welding of duplex stainless steels, reheating by subsequent passes causes a progressive increase of

Recommended for publication by Commission IX—Behaviour of Metals Subjected to Welding.

✉ Elin M. Westin
elin.westin@voestalpine.com

¹ voestalpine Böhler Welding Austria GmbH,
Böhler-Welding-Str. 1, 8605 Kapfenberg, Austria

Table 1 Typical chemical composition for selected duplex stainless steel base materials

EN	ASTM	C	Cr	Ni	Mo	N	Others
1.4162	UNS S32101	0.03	21.5	1.5	0.3	0.22	5Mn
1.4062	UNS S32202	0.03	22.0	3.0	0.3	0.20	2Mn
1.4362	UNS S32304	0.02	23.0	4.8	0.3	0.10	
1.4462	UNS S31803	0.02	22.0	5.7	3.1	0.15	
1.4462	UNS S32205	0.02	22.0	5.7	3.1	0.17	
1.4507	UNS S32550	0.02	24.9	5.4	3.1	0.17	2Cu
1.4410	UNS S32750	0.02	25.0	7.0	4.0	0.27	
1.4501	UNS S32760	0.02	25.4	6.9	3.8	0.27	W
1.4477	UNS S32906	0.02	29.0	7.0	2.3	0.35	0.6Cu

Table 2 Typical chemical compositions for selected duplex stainless steel filler metals

Type	Process	Standard	C	Si	Mn	Cr	Ni	Mo	N	Others
ER2307	Solid wire	AWS A5.9	0.02	0.4	0.5	23.0	7.0	0.3	0.14	
ER2209	Solid wire	AWS A5.9	0.02	0.4	1.7	22.5	8.8	3.2	0.15	
ER2594	Solid wire	AWS A5.9	0.02	0.4	0.4	25.0	9.5	4.0	0.25	
ER2595	Solid wire	AWS A5.9	0.02	0.3	0.8	25.3	9.5	3.7	0.22	0.6Cu, 0.6 W
E2307TX-X	FCAW	AWS A5.22	0.02	0.7	1.1	24.6	9.0	0.4	0.14	
E2209TX-X	FCAW	AWS A5.22	0.02	0.7	0.9	22.8	9.0	3.2	0.13	
E2594TX-X	FCAW	AWS A5.22	0.02	0.7	0.9	25.3	9.8	3.7	0.23	
E2307-XX	SMAW	AWS A5.4	0.02	0.8	0.7	23.5	7.4	0.3	0.12	
E2209-XX	SMAW	AWS A5.4	0.02	0.8	0.8	22.6	9.5	3.1	0.16	
E2594-XX	SMAW	AWS A5.4	0.02	0.8	0.9	24.8	9.7	3.6	0.23	
E2595-XX	SMAW	AWS A5.4	0.02	0.5	0.9	25.8	8.6	3.9	0.24	0.7Cu, 0.9 W

austenite and the morphology changes [17–22]. This occurs mainly as growth of primary austenite and by precipitation of secondary austenite in prior weld beads [23, 24]. The largest dilution from the parent material takes place in the root pass and the ferrite content here reaches its maximum [19, 20]. As the filler metal is over-alloyed in nickel and the dilution from the base metal decreases when previous beads are partly remelted, the austenite fraction increases when adding more weld passes. As the maximum temperature obtained from the thermal cycle by a subsequent run is a function of the distance, the ferrite and austenite balance can vary significantly within one single pass. Reheating of previous passes appears to have the largest influence on the final weld metal austenite content as the last weld bead has again high ferrite content, because it is not reheated by any other passes [19, 20].

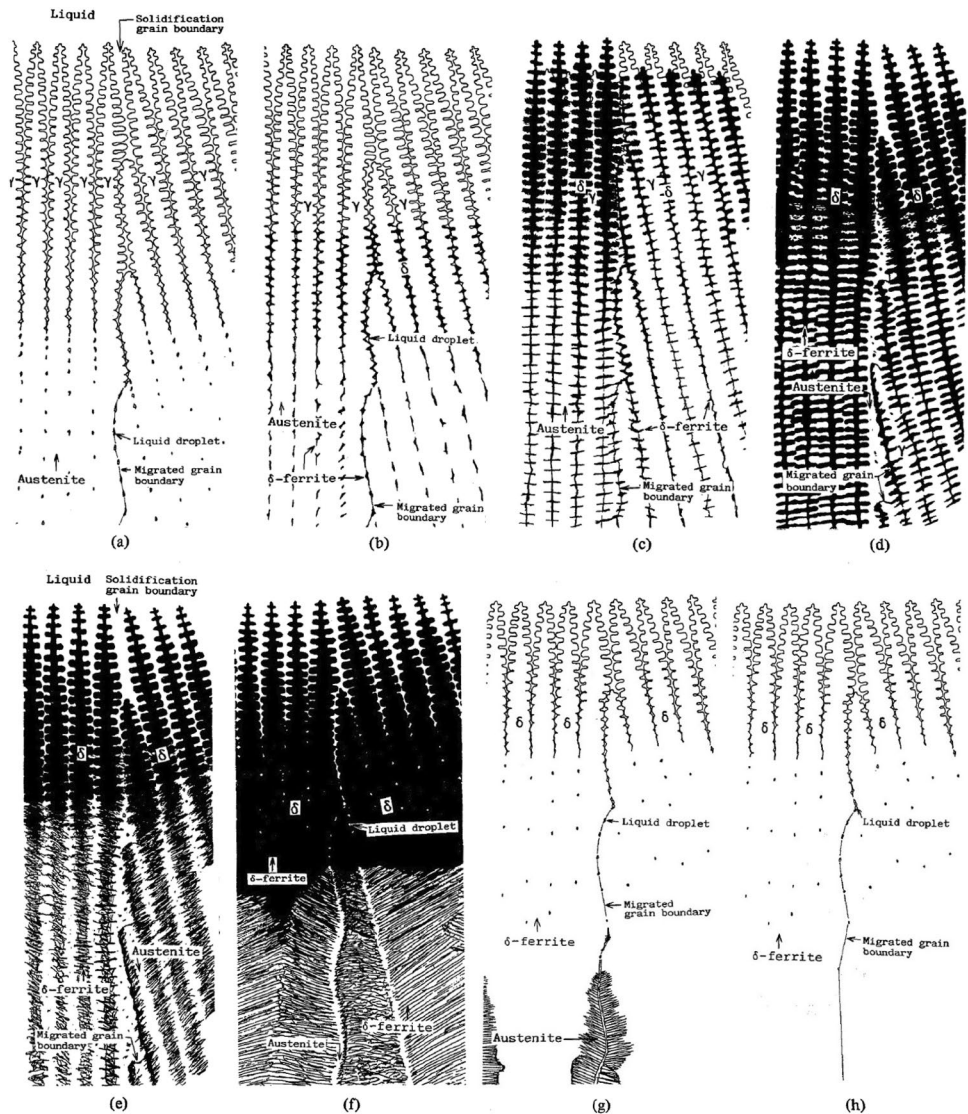
2 General solidification

Weld solidification occurs as epitaxial growth of the ferrite grains along the fusion boundary and is oriented in relation to the thermal gradient [25]. Dendritic growth in body centered cubic materials takes place in the $\langle 100 \rangle$ direction [4, 26]. The element distribution in the dendrites is primarily

affected by the chemical composition, the temperature gradient in the liquid adjacent to the solid–liquid interface, and to some extent to the growth rate of the solid [1, 27, 28]. Figure 1 shows different solidification modes observed in weld metals [29]. Duplex stainless steels solidify as fully ferrite and grain boundary and Widmanstätten austenite form upon cooling.

Segregation of residual impurities or intentional alloying elements to boundaries may lower the solidus temperature [30]. This type of segregation does take place in the fusion zone of duplex stainless steels, but the levels are appreciably lower than those observed for austenitic solidification [31]. The partitioning of the metallic elements between the ferrite and austenite phases is not as prominent in the weld metal as in the base metal, but often follows the dendritic solidification structure [1, 32, 33]. Nitrogen on the other hand is partitioned and enriched in the austenite to a greater extent than in the parent material, while some preferential partitioning of chromium may occur in the ferrite [1, 6, 34]. The mode of solidification is readily detectable by metallographic examination of the solidified weld metal [27], but cellular dendrites and dendrites are generally not apparent in the fusion zone of duplex stainless steels using conventional metallographic techniques. The segregation pattern and dendrites are not visible as the microstructure is largely

Fig. 1 Solidification and solid-state transformation behavior and characteristic morphologies **a** fully ferritic, **b** intercellular eutectic ferrite, **c** eutectic ferrite, **d** vermicular ferrite, **e** lacy ferrite, **f** acicular ferrite, **g** Widmanstätten austenite, and **h** fully ferrite. From Katayama et al. [29]. Courtesy of the Japanese Welding Institute



controlled by the distribution of nitrogen [1]. The rapid diffusion in ferrite relative to austenite is also responsible for the absence of apparent cells and dendrites.

3 Solidification cracking

Although the terminology “hot cracking” actually includes other phenomena such as reheat, liquation, and ductility dip cracking, the wording is commonly used for the solidification cracking dominating in stainless steel welds. Weld solidification cracking is caused by a combination of thermomechanical and metallurgical aspects [35]. In stainless steels, it requires the presence of a crack-susceptible microstructure, which forms at the final stage of solidification due to the presence of low-melting, impurity enriched liquid films [2]. It has been suggested to appear at the solidification

end inside the mushy zone (the region where dendrites and liquid coexist) that is subject to shrinkage and thermal contraction and where the semi-solid shows little ductility in the terminal stage of solidification [36]. In aluminum and nickel-base alloys, cracking is rather caused by segregation of elements forming low-melting eutectic films [37, 38]. Figure 2 shows the surface of a solidification crack with dendritic solidification pattern in 100× magnification.

Cracking occurs when the tensile stresses developed across the adjacent grains exceed the strength of the almost completely solidified weld metal [4]. It is assumed cracking can occur if volumetric shrinkage exceeds volumetric feeding [39]. The threshold level of both strain and interdendritic liquid necessary to cause cracking is material specific and depends to a large extent on both the composition of the material and the welding conditions [40, 41]. The solidification cracking susceptibility of a material (the interval

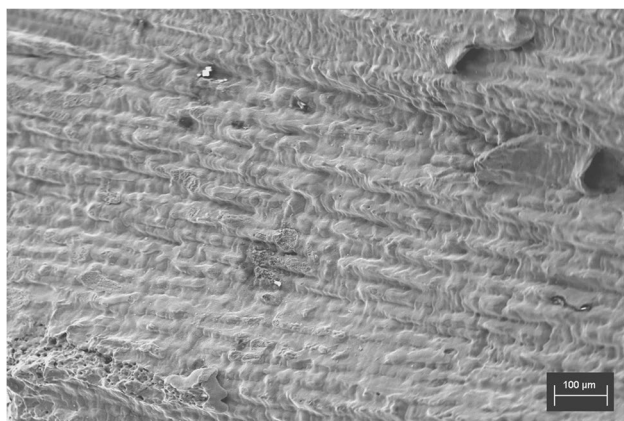


Fig. 2 Solidification crack showing dendritic solidification pattern — duplex stainless UNS S31500 welded with the submerged arc welding (SAW) process

of temperatures over which solidification cracking is likely to occur) can be described by its so-called brittleness-temperature-range (BTR) or solidification cracking temperature range (SCTR) [42]. A wide solidification range may permit a large build-up of strain and a greater probability to crack [43]. Critical strains and strain rates may serve as a driving force for solidification crack formation for a given microstructure and solidification conditions [44]. A more recent approach is that the strain rate actually plays the most important role [44, 45]. Cracking may be initiated at metastable pore nuclei, oxide films, or gas trapped in the vicinity of oxides [39].

Particularly sulfur and phosphorus promote hot cracking by lowering the solidus temperature and lengthening the BTR, and the risk increases if the solidification occurs as primary austenite [46–48]. Kujanpää et al. [49] created the diagram in Fig. 3 indicating that the weld solidification cracking can be predicted from the weld metal composition.

It is generally believed that the concentration of these impurities at the grain boundaries of austenitic stainless steels and thus their damaging effect on solidification cracking can be reduced if δ -ferrite is present in significant amounts [29, 50–52]. Yu et al. [53] have suggested that to understand solidification cracking in austenitic stainless steels, revealing the elevated temperature microstructure of the mushy zone during welding is much more useful than examining the room-temperature microstructure of the fusion zone after welding. When welding, both tensile and compressive stresses are present during the solidification due to non-uniform thermal distribution and other mechanical restraints. According to the authors, the solidification cracks normally do not appear in the mushy zone itself, but at somewhat lower temperatures. The austenitic stainless steel 310 has higher susceptibility to hot cracking than 304.

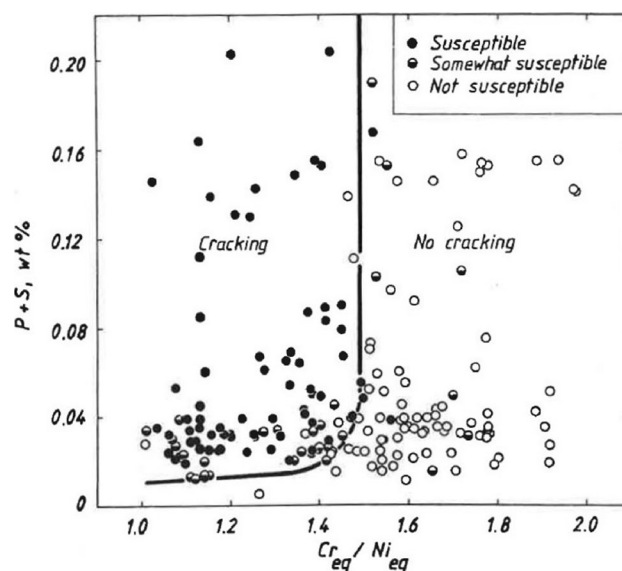


Fig. 3 Effect of sulfur and phosphorous and the Cr_{eq}/Ni_{eq} on solidification cracking. From Kujanpää et al. [49]

The authors concluded that the mushy zone is significantly wider in 310 than 304, and that the coarse and long γ dendrites having straight boundaries help liquid films remain continuous and cracks can propagate.

It is well established that the susceptibility of austenitic stainless steels is much lower when the primary solidification phase is δ -ferrite than when the primary phase is austenite [4, 41, 49, 54, 55]. Hull [54] proposed that the optimum cracking resistance with 5–10% δ -ferrite resulted from the presence of a significant austenite/ferrite interfacial area during the final stages of solidification. The crack propagation would thus be halted due to the lower surface energy, inhibiting interdendritic boundary wetting by low-melting liquid films. In addition, less solidification shrinkage and thermal expansion contribute to a reduced crack risk [56].

Suutala et al. [34] correlated the cracking susceptibility in a wide range of stainless steels with a Cr_{eq}/Ni_{eq} ratio. At low ratio values, the primary solidification occurred as austenite and the risk for cracking was high. Above a threshold value of Cr_{eq}/Ni_{eq} , the primary solidification shifted to ferrite and the cracking sensitivity decreased. In welds exhibiting more than 30% ferrite, including modern duplex stainless steels, the solidification would be entirely ferritic, and interdendritic liquid films would be more likely to wet the ferrite/ferrite boundaries. Kujanpää et al. [49, 57, 58] suggested that there exists a cracking susceptibility “valley” optimized for Cr_{eq}/Ni_{eq} ratios in the vicinity of 1.5–2.0 solidifying in a ferritic/austenitic mode. Further studies have confirmed that there is a minimum in solidification crack sensitivity at a ferrite level of 5–20% [27, 29, 31, 41, 59–61]. Lippold

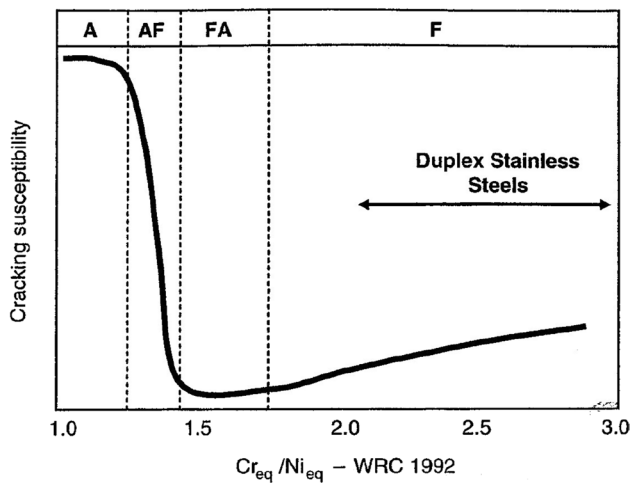


Fig. 4 Vareststraint test data for different solidification modes obtained in different austenitic and duplex stainless steels. From Lippold and Kotecki [47]

and Kotecki [47] confirmed these findings for austenitic and duplex stainless steels (Fig. 4).

The dilution from the base metal influences the δ -ferrite content in the weld metal and the final content of impurities, and can be controlled by limiting the heat input and optimizing the joint preparation. The choice of welding method and filler metal can further affect the amount of alloying elements, impurities, and oxides. Cieslak et al. [62] concluded that also a too long stick-out or arc length may cause nitrogen pick-up in austenitic stainless steels and increase the hot cracking susceptibility.

4 Detection of hot cracks and the effect on properties

Solidification cracking mostly take place in the root pass or in the last weld bead, as for example, crater cracks or center cracks, while reheat or liquation cracking can occur in previously deposited weld metal as a result of secondary phases and thermal strain. Figure 5 shows a rare case of liquation cracking in the HAZ and across the fusion line of a lean duplex UNS S32101 after stationary (non-moving) welding with the GTAW process for 20 s. These cracks are suspected to have been caused by liquation of low-melting phases in the grain boundaries together with large strains. The critical local strain rates are related to specific thermal, material, and restraining conditions, which are in turn influenced by factors such as the plate thickness, material strength, and joint preparation, restraint and welding parameters affecting the weld bead shape [63, 64]. Methods for testing the susceptibility to hot cracking have been reviewed by Kannengiesser and Böllinghaus [65].

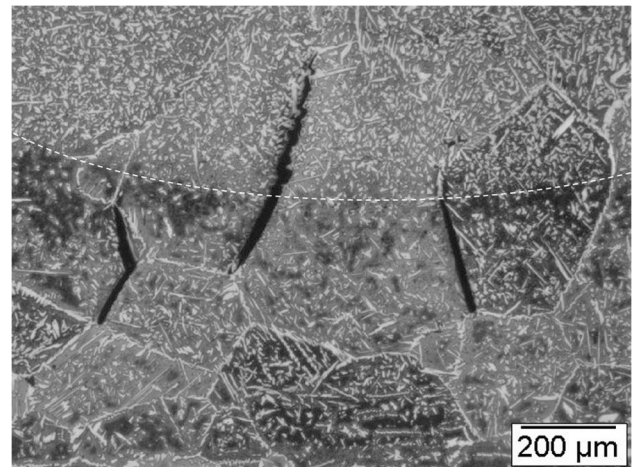
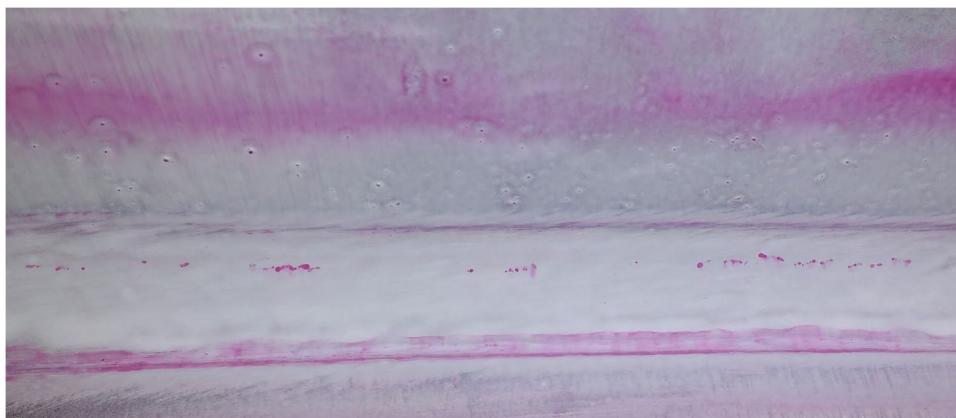


Fig. 5 Liquation cracks in 6-mm UNS S32101 stationary welded for 60 s with the GTAW process using Ar+5% N₂ as shielding gas. The sample was polished to 3 μm using SiO₂ in the last step and etched in Beraha II

Solidification cracks may be challenging to detect using non-destructive techniques. Dye-penetrant testing can locate surface breaking cracks and cracks located near the surface could become visible after grinding (Fig. 6). Small irregularities without voids can probably not be found with radiographic or ultrasonic testing, while slightly larger cracks may become discernible with special instruments and procedures. The smallest cracks would possibly only be detected in a metallographic examination of polished cross-sections, but as the cross-section is rather arbitrary, it is more likely to identify continuous than shorter cracks. Welded joints can be subject to different types of bend testing. If no irregularities are located in the cap layer, the face out bend test will pass. Root out bend testing of V-joints could fail in case cracks go through most of the root bead. Sidewall bend testing can, on the other hand, be highly efficient to open and detect small cracks in cross-sections of welds. ASME IX [66] sets the defect size limit to 3.2 mm on side bend testing. Another way to find and inspect solidification cracks is to examine the fracture surface after impact toughness testing. If present, the dendritic solidification structure of larger cracks may be visible to the naked eye, while small cracks probably require examination with a light optical or scanning electron microscope.

Surface breaking cracks are particularly important to find as they can have a negative effect on the corrosion resistance, mechanical properties, and fatigue. Sub-surface solidification and liquation cracks may not affect the service performance, because of their small size and favorable location, but in certain circumstances, they may contribute to premature failure [30]. It may not be possible to pass corrosion testing of welds including end grains, and the creep

Fig. 6 Irregularities visible with dye-penetrant testing after grinding the surface of a fillet weld in 30-mm UNS S32205 welded with the FCAW process using an E2209T0 type of wire



strength may be reduced, but the effect on other mechanical properties would usually be low [67–69].

5 Effect of chemical composition

The literature gives some indications which elements can be of importance for limiting the hot cracking sensitivity. Ogawa and Tsunetomi [70] concluded that the hot cracking resistance of austenitic stainless steels can be improved by reducing phosphorous and sulfur to <0.002 wt.-%, decreasing silicon, increasing carbon when niobium is high, and increasing nitrogen when niobium is absent. The authors concluded that niobium and phosphorous have a detrimental effect on fully austenitic weld metal, since the hot cracking susceptibility increases considerably when the niobium content exceeds 0.03 wt.-% and phosphorous 0.015 wt.-%. Also silicon was identified as an element influencing the total crack length, where the resistance decreased linearly up till approximately 1.5 wt.-%, but when delta ferrite was present, silicon was on the contrary positive. Other elements, which can have a negative influence, are hafnium, zirconium, boron, and copper.

Matsuda et al. [52, 71–79] published an extensive series of papers on hot cracking sensitivity of austenitic stainless steels. The authors concluded that welds solidifying as delta-ferrite have a greater solubility for impurities [52]. Segregation of sulfur, phosphorous, silicon, and manganese as phosphides and sulfides was observed in the grain boundaries of SUS 304 and 310S weld metal [71, 75]. The sulfides enriched in manganese and chromium and depleted in iron and nickel were present in a granular or rod-like shape [71]. The melting point of manganese sulfide (MnS) in SUS 304 weld metal was measured to 1280–1310 °C [72]. Sulfur was suggested to widen the BTR by segregation. Sulfur also segregates more in SUS 304 weld grain boundaries than phosphorous [75]. The melting point of the observed phosphides was estimated at 1060–1100 °C [72]. Segregation of sulfur was concluded to more easily take place along the

cellular dendritic and columnar grain boundaries in SUS 310S weld metal with primarily austenitic solidification than SUS 304 weld metal with primarily ferritic solidification [71]. To reduce the hot cracking sensitivity of the fully austenitic stainless steel SUS 310S, it was beneficial to decrease the phosphorous and silicon contents and to add manganese to bind sulfur as MnS [72]. For a phosphorous content of 0.02–0.03 wt.-% and a sulfur content exceeding 0.005 wt.-%, 6% manganese would be required to make a SUS 310S weld metal resistant to solidification cracking [77]. The sulfur and phosphorous contents were overshadowed by the solidification mode, where SUS 304 solidifying as primary ferrite was considerably less susceptible than the fully austenitic SUS 310S. The negative effect of nitrogen on the hot cracking resistance of SUS 304 weld metal was assigned to the decrease in delta ferrite and hence increased microsegregation of particularly phosphorous [78]. Titanium was suggested to increase the solidification temperature of phosphide eutectics [79].

Figure 7 shows solidification cracks formed in UNS S32205 with 0.017 wt.-% sulfur welded with the submerged arc welding (SAW) process. The cracks caused by high sulfur content combined with fairly large heat inputs were detected by dye-penetrant testing after machining.

There are also reports where additions of cerium, lanthanum, and rare earth metals have been identified to have a positive effect on the solidification crack susceptibility [76, 80, 81]. Matsuda et al. [76] found that controlled lanthanum and REM additions could reduce the BTR in UNS S310S weld metal with 0.03 wt.-% phosphorous and 0.05 wt.-% sulfur. Lanthanum was identified to react with sulfur and oxygen during melting and casting. Both desulfurization and oxidation could be confirmed, but the amount of phosphorous remained unaffected. In addition, lanthanum increased the solidification temperature of MnS and M_3P by formation of oxysulfides, LaS and LaP. The optimum lanthanum content was suggested to be $La = 4.5P + 8.7S$. Yamada et al. [80] used rare earth metals to immobilize

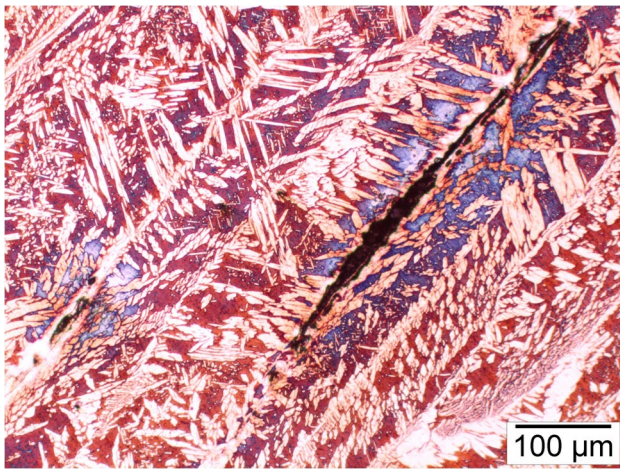


Fig. 7 Light optical micrograph of 0.3- and 1-mm-long solidification cracks found in a free-machining UNS S32205 grade welded with the SAW process and a wire of ER2209 type (Etchant of Beraha II type)

sulfur and argued that the effect becomes higher when the total content exceeds that of the sulfur content. Gong et al. [81] investigated the effect of 0.005% and 0.02% cerium to UNS S32101 duplex stainless steel base material. Large size and irregular inclusions of $\text{Al}_2\text{O}_3\text{-MnS}$ and Al_2O_3 could be modified, refined, and spheroidized by cerium into small size and spherical CeAlO_3 , $\text{Ce}_2\text{O}_3\text{S}$, and Ce_2O_3 . The cerium-containing inclusions were identified to reduce the likeliness of crack initiation and propagation and increase the mechanical properties of the parent metal.

All impurities that segregate at the grain and solidification boundaries decrease the hot workability of austenitic stainless steel; lead, bismuth, and sulfur are among the most harmful elements [82, 83]. Tehovnik et al. [84] performed hot bending tests on austenitic stainless steel with 0.0083 wt.-% lead and showed that droplets of lead enriched at the solidification boundaries caused hot cracking. Walsh and Andersson [85] evaluated the effect of trace elements in a series of nickel-base alloys. They found evidence of grain boundary segregation of sulfur, bismuth, tellurium, and lead. At 26-ppm bulk lead levels, a globular constituent of essentially pure lead was detected in the grain boundaries. Bergh [86] concluded that amounts as low as 0.004 wt.-% lead can drastically affect the hot workability of austenitic stainless steel grades, by precipitation of lead particles in the primary grain boundaries. Jensfeld and Norrman [87] reported that 0.002–0.003 wt.-% lead and as little as 0.0005 wt.-% bismuth produced cracking during hot forging of type 316 austenitic stainless steel. The fracture occurred along the primary grain boundaries where the cohesion was reduced by the presence of bismuth. Bismuth was identified as a contamination in a single delivery of ferromolybdenum. The reason for bismuth being more detrimental than lead was suggested to

be related to the efficient wetting of grain boundaries and dendrites by bismuth and bismuth-rich low melting phases.

Cole and Richardson [88] demonstrated that the trace elements bismuth, lead, and antimony segregate strongly to the grain boundaries and reduce the grain boundary cohesion. Ljungström [89] investigated the influence of bismuth, lead, tin, antimony, and arsenic on the ductility of type 316L using hot tensile testing and found a negative effect with increasing content of trace elements. Based on this work, Norström [90] proposed an embrittling parameter expressed as the lead equivalent $\text{Pb}_{\text{eq}} = \% \text{Pb} + 2 \times \% \text{Bi} + 0.5 \times \% \text{Te} + 0.03 \times \% \text{Sb} + 0.02 \times \% \text{Sn} + 0.01 \times \% \text{As}$. Skoglund [91] performed a similar study on the influence of trace elements on the hot ductility of type 316L stainless steel and adjusted the expression with a factor of 4 for bismuth to $\text{Pb}_{\text{eq}} = \% \text{Pb} + 4 \times \% \text{Bi} + 0.02 \times \% \text{Sb} + 0.01 \times \% \text{Sn} + 0.007 \times \% \text{As}$. The type of ore and source of other raw materials may play a role, as for instance lead is a contamination that could originate from the strip material, powder metals, and slag formers as well as intentional bismuth addition. The same applies for other trace elements such as tellurium, antimony, tin, and arsenic. None of these is listed on the certificate from the manufacturer and probably also not included in the typical analysis from the accredited laboratory measuring the all-weld metal composition, unless extra specifying it when placing the order.

6 Solidification cracking in duplex alloys

Duplex stainless steels are generally resistant to solidification cracking due to fully ferritic solidification [92]. The prior ferrite/ferrite grain boundaries dissolve some of the impurity elements originating both from the parent material and filler metal additions. Not many research results regarding fusion zone cracking have been published for the duplex grades specifically, as the experience with a number of commercial duplex stainless steels with ferrite contents of 20–80% does not indicate that weld solidification cracking is a significant problem [41, 92].

Historically only a few studies of hot cracking in duplex alloys have been published [3, 31, 41, 59, 93–95]. Gooch and Honeycomb [3, 95] reported that solidification cracks have been found in duplex stainless plates above about 10-mm thickness with the shielded metal arc welding (SMAW), gas metal arc welding (GMAW), and SAW processes. Matsuda et al. [27] used modified duplex stainless SUS 329J2L (UNS S31803) types of metal-cored wire to vary the ferrite content from 0 to 85%. The highest resistance to solidification cracking was found between 5 and 20% ferrite. Below 5%, the susceptibility to hot cracking increased rapidly, and above 20%, it increased gradually. Nelson et al. [41] found a slight increase in susceptibility

at high strain rates for duplex stainless steels as compared to 304L type alloys and drew the conclusion that duplex grades may experience problems in applications where the weld restraint is high. The greater cracking proneness of the commercial duplex alloys was suggested to be caused by formation of a complex, low-melting liquid film enriched in copper and phosphorous. Varol et al. [31] investigated the fusion zone solidification cracking susceptibility of alloy SAF 2205 to commercial austenitic stainless steels. Results obtained indicate that the duplex stainless steel was more resistant to weld solidification cracking than type AISI 304 and AISI 316 alloys with fully austenitic solidification, but more prone than AISI 304 and AISI 316 alloys showing ferritic solidification. Results by Matsuda et al. [59], Varol et al. [31], and Nelson et al. [41] were consistent with those previously reported by Kujanpää et al. [49, 57, 58], who showed an increase in **solidification cracking** susceptibility at high Cr_{eq}/Ni_{eq} ratios.

Most papers on solidification cracking were on earlier generations of duplex stainless grades, before the positive effect of nitrogen was clarified. This means that the references here [3, 31, 41, 49, 58, 59, 93–95] published between 1977 and 1989 were on duplex weldments with rather high ferrite content. The duplex alloys were low in nitrogen and the resulting microstructure showed large ferrite grains with precipitates such as chromium nitrides and carbides. Austenite was found in the grain boundaries, but there was limited formation of Widmanstätten austenite based on the published micrographs.

For modern duplex stainless steels, few recent contributions on solidification cracking have been found. Karlsson [96] observed solidification cracking in UNS S32205 material welded with SAW, laser, and laser hybrid processes and these were related to very shallow beads or essentially ferritic welds. In the case of SAW, the cracks were found in thin beads forming wings on the side and these could be counteracted by modifying the bead profile. The laser and laser-hybrid welds had considerably higher ferrite content and the solution was suggested to modify the welding procedure to allow for more austenite formation.

Fellman and Westin [97] performed fiber laser gas-metal arc (GMA) hybrid welding of 8-mm UNS S32205 stainless steel with ER2209 solid wire as filler metal. With leading laser, the filler metal penetration was shallow and the ferrite content 84–91%. Solidification cracks were formed on the sides in the upper part of the weld having a wide, but rather thin shape (Fig. 8). Bend testing detected these defects and tensile testing showed failure in the weld metal. With trailing laser configuration, the weld penetration became more uniform and the austenite formation improved considerably with 67–82%. These samples did not show any evidence of cracking, passed the bend test, and failed in the parent material when subject to tensile testing. It was concluded

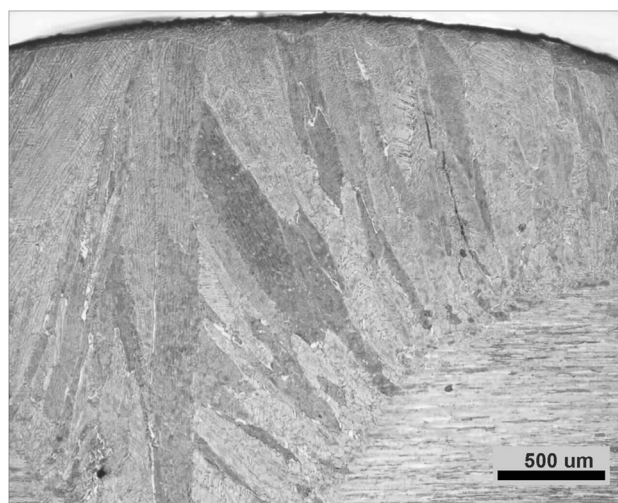


Fig. 8 Solidification crack found in the grain boundaries of GMA-laser hybrid welded UNS S32205 with an ER2209 solid wire

that the GMAW process controlled the weld shape in the leading laser configuration; the welding speed was too high and cracks formed in the outer parts of the weld due to rapid cooling and large tensile stresses.

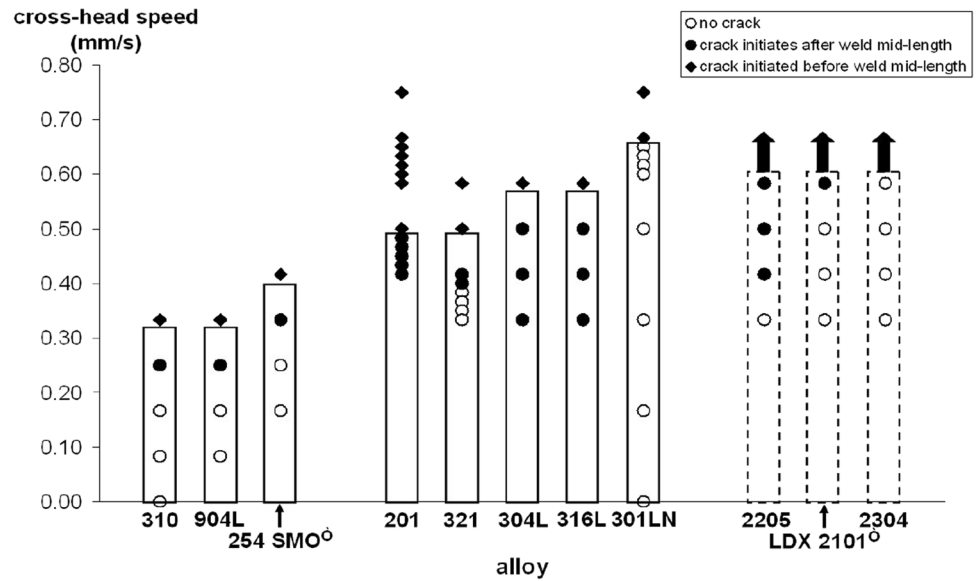
Cross et al. [98] used the controlled tensile weldability (CTW) test to rank 11 different austenitic, superaustenitic, and duplex stainless grades as to their relative laser weldability. Together with the austenitic AISI 301LN alloy, the lean duplex grades UNS S32101 and UNS S32304 showed the highest resistance to cracking (Fig. 9). The susceptibility of the standard duplex UNS S32205 was confirmed to be somewhat lower than for AISI 304L and AISI 316L.

Jadav et al. [99] deposited ER2209 filler wire with the GTAW process using 100% Ar and Ar + 2% N₂ as shielding gas. They performed transverse testing and concluded that apart from a crack in one single sample performed with nitrogen additions to the shielding gas, the duplex alloy was resistant to solidification cracking also at higher degrees of strain.

Saida and Ogura [100] studied hot cracking susceptibility of modern alloys subject to GTAW and laser welding. It was concluded that standard, lean, and superduplex grades were as resistant to solidification cracking as austenitic stainless steels solidifying in ferritic-austenitic mode and more resistant than austenitic alloys with austenitic-ferritic or fully austenitic solidification. The improved cracking resistance was suggested to be attributed to suppression of segregated phosphorous, sulfur, and carbon.

A so far unpublished German study [101] compared different ER2209 filler wires for welding with the SAW process. It was decided that the wires with higher silicon and sulfur content for improved fluidity with the GMAW process were not as suitable for SAW due to formation of hot cracks.

Fig. 9 Comparison of CTW test results for super-austenitic, austenitic, and duplex stainless steels showing observed solidification cracking behavior varying with applied cross-weld displacement rate (i.e., cross-head speed) [98]



Instead, it was recommended to use sulfur-free wires with controlled silicon content and a more basic type of flux.

Surface cracks have been observed in stationary welding using the GTAW process with Ar+2–8% N₂ [102]. In addition to the shrinkage crater naturally formed, the combination of a non-moving arc and nitrogen additions to the shielding gas changed the surface structure (Fig. 10). Over-saturation of nitrogen can lead to excessive amounts of austenite at the surface, which can cause solidification cracking similar to that seen for fully austenitic solidification [49, 57]. The longer arc length of 5 mm in Fig. 10a combined with as much as 8% nitrogen in the shielding gas inevitably led to absorption of excessive amounts of nitrogen after 60 s, but similar observations could also be made for more standard settings with 2.5-mm arc length and 2% nitrogen (Fig. 10b). Another possible explanation could be discontinuous precipitation of chromium nitrides reported to cause intergranular cracking in high-nitrogen austenitic stainless steels [103–105]. This type of microstructure called false nitrogenous pearlite has also been observed in regular GTAW of

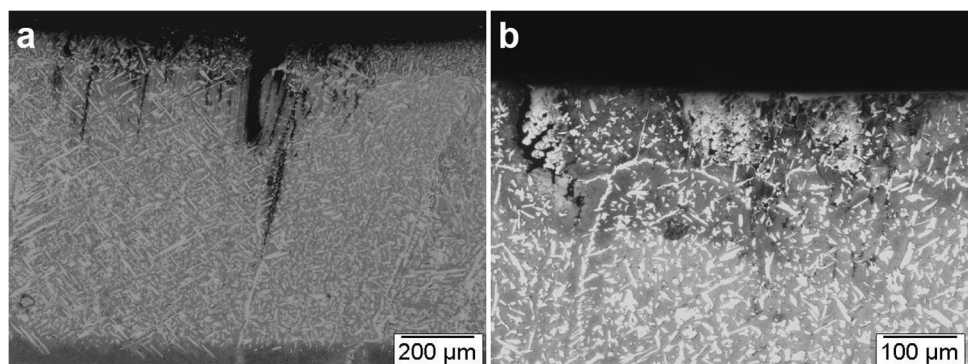
the hyper duplex grade UNS S32906 with Ar+2% N₂ and caused a clear reduction in the corrosion performance [106].

7 Particularities in the FCAW process

7.1 Rapid welding speed

Rapid welding is possible with the flux-cored arc welding (FCAW) process and it is often selected to increase the productivity. The complexity with welding speed has been reviewed in detail by Coniglio and Cross [36, 107, 108]. The majority of the published studies are on alloys known to be susceptible to solidification cracking and tested using GTAW (re)melting. At higher welding speeds, the weld puddle becomes shaped more as an elongated teardrop and may be more susceptible to hot cracking than one that is rounded [109, 110]. Affecting not only the weld pool shape, but also the cross-sectional area, the travel speed has been reported to influence solidification cracking formation through both thermal and metallurgical effects [36]. Morgan-Warren and

Fig. 10 Surface cracks in the center of stationary arc (non-travelling) welds, welded for 60 s using the GTAW process with **a** 5-mm arc length and Ar+8% N₂, and **b** 2.5-mm arc length and Ar+2% N₂ (Beraha II etchant)



Jordan [111] suggested that increasing welding speed deteriorates the solidification crack resistance when keeping the weld bead shape constant.

Various flux-cored wires show different weldability and could allow or force the welder to weld slightly in another way. Manual welding can normally lead to small variations in welding speed, stick-out, arc length, and gun manipulation. These parameters can have an influence on the sensitivity to solidification cracking.

7.2 Ceramic backing

The ceramic backings are used to ensure safe penetration by allowing welding in wider gaps and act as support for the welder. The productivity can be optimized with a good root finish. There is according to Chen [112] increased risk for solidification cracks in PA/1G position when welding against ceramic backing where wide, thin passes may crack due to high shrinkage stresses imposed on small and convex weld throats. To avoid cold laps, the welder typically increases the current, which results in a larger melt and need to weld faster. This is from a production point of view highly beneficial, but the risk for solidification cracking increases accordingly as the weld becomes convex and thinner in the middle. It may be necessary to reduce welding currents for particularly critical seams [113]. By welding slower on ceramic backings with a lower voltage and wire speed, it is possible to build up a more concave weld to gain strength in the center of the root. Figure 11 shows a hot crack detected with a duplex flux-cored wire in a modified version of the FISCO test against ceramic backing [114].

Copper backing strips are preferred over ceramic backings from a cracking point [113]. When metal plates are used as backing, there is an additional cooling effect on the root (heat dissipation), which potentially affects the solidification behavior. Although being slower, GTAW may be the best

process for welding the root combining higher resistance to solidification cracking with better impact toughness and corrosion performance.

7.3 Ferrite content resulting from flux-cored arc wires

A requirement of the phase balance is common for welding procedures when welding duplex stainless steels. The ferrite content in the weld metal is normally specified at 30–70% [115] or stricter with 35–65% [116–119]. An average ferrite content outside the limits set for the phase analysis may affect the mechanical properties and corrosion performance. It is generally accepted, however, that the ferrite content is not a property itself, but should serve as an indication of the effect on the corrosion performance and mechanical properties [120].

As a slag forming process, FCAW with more oxides and inclusions inherently show lower impact toughness than gas welding with solid wires. The acceptance criteria in ISO 17781 [121] divide the minimum absorbed energy at $-46\text{ }^{\circ}\text{C}$ for duplex stainless steel in as-welded condition in two quality levels. The most common requirement, quality level QL II, is sufficient for most applications and requires a mean minimum energy of 35 J, with no sample below 27 J. To fulfil the strictest quality level QL I, the minimum mean energy needed is 50 J and min. 40 J for a single sample. To improve the toughness, wire manufacturers may adjust the chemical composition of the weld metal to result in a microstructure with somewhat more austenite. As discussed earlier, the austenite content increases with more weld layers.

When welding stainless steel with flux-cored wires, Ar + 18–25% CO₂ is the shielding gas that produces the best results and the greatest slag control. Mixed gas has a very positive influence on arc stability, producing a fine, spatter-free droplet transfer. It is also possible to use 100% CO₂,

Fig. 11 Solidification crack detected with a duplex flux-cored wire in a modified version of the FISCO test, where rapid welding can be performed against ceramic backing [114]



but the voltage needs to be increased by 2–3 V to achieve the correct arc length. The main advantage with pure CO₂ is that it provides deep weld penetration, which is useful when welding thick material. It may also be more forgiving for unexperienced welders. The process runs hotter, which can be a benefit, but at the same time makes it more challenging to weld thin plates or out-of-position. Moreover, it produces more welding fumes and the surface becomes more oxidized [122]. Use of pure CO₂ as shielding gas is known to lead to element loss and a slight increase in weld metal austenite content [123, 124]. This can affect the mechanical properties and the corrosion resistance.

In multipass welding, also the heat input and the inter-pass temperature have an influence. At lower cooling rates, there is more time for transformation from ferrite to austenite and the width of the austenite at ferrite grain boundaries becomes wider [15, 16]. Li et al. [125] studied the flux-core arc welding process for welding UNS S32205 and concluded that the ferrite content increases with the increase of welding speed and torch angle, but decreases with the increase of welding current and welding voltage. Palpandi et al. [126] studied the effect of welding parameters for an E2209T1-1/4 flux-cored wire with mixed gas on ferrite content and mechanical properties and found the optimized heat input to be 1.5 kJ/mm.

Suutala et al. [34] concluded that in welds exhibiting 30% ferrite, including modern duplex stainless steels, the solidification would be entirely ferritic, and interdendritic liquid films would be more likely to wet the ferrite/ferrite boundaries. Depending on the resulting BTR of low melting films and the solidification range of the slag, the duplex alloys may become more susceptible to solidification cracking. Where hot cracking has been reported, the condition with straight ferrite grain boundaries is typically fulfilled [31, 41, 59, 96, 97]. In the previous generations of duplex stainless steels, the nitrogen content was lower. The austenite formation in the grain boundaries thus occurred at a later stage. With the modern wires, the austenite precipitates earlier, which increases the risk that the low-melting phases are still molten in the austenite. The face centered cubic structure is more sensitive to wetting of the boundaries and this may be of significance as the low-melting films responsible for solidification cracking may still be liquid at the temperatures where grain boundary austenite has precipitated in long and straight ferrite grain boundaries.

7.4 Restraint and welding parameters

Kou [127] stated that the risk for solidification cracking is determined by the solidification temperature range, the amount and distribution of liquid at the terminal stage of solidification, the surface tension of the grain-boundary

liquid, the ductility of solidifying weld metal and the tendency to weld metal contraction and the degree of restraint. From the literature review and experience shared by welding companies, the worst possible welding conditions for solidification cracks are high restraint and especially when welding against ceramic backing.

Nelson et al. [41] concluded that duplex grades may experience problems in applications where the weld restraint is high. Liljas [56] stated that hot cracking might occur also in duplex stainless steels in highly restrained constructions, e.g., heavy sections. Karlsson [96] made a similar statement saying that in rare cases, preheating to maximum 150 °C is used to minimize the risk of cracking when welding thick and/or heavily restrained work pieces with low arc energy to reduce cooling rate and stress levels. Kou [39] defined that the more tightly the work piece is clamped down or connected to a rigid body, the more tensile strain is induced by its thermal contraction. Sterjovski et al. [128] used the pulsed tandem-GMAW process for welding naval hull steels and concluded that the risk for solidification cracking increased with the weld bead depth:width ratio and joint restraint with increasing plate thickness.

Although being generally resistant, duplex stainless steels can under certain circumstances be subject to solidification cracking. The susceptibility increases when thick material is welded under full restraint. The FCAW process can make the situation more complex as the root pass is often made against a ceramic backing. Due to a large melt, high welding speed, and long molten weld pool, a normally resistant flux-cored wire with a certain slag concept and chemical composition may become prone to cracking. The risk may increase if 100% CO₂ is used as shielding gas.

7.5 Bismuth additions

Godai et al. [129] patented bismuth additions to stainless flux-cored wires in 1982, where it was suggested that the oxides of lead, bismuth, and antimony can be added to a siliceous slag system to obtain very clean welds and improve the slag removal. A majority of today's flux-cored arc wires are still alloyed with bismuth to improve the slag detachability. Bismuth acts as a surface-active element and lowers the surface tension of molten metal [130]. Bi₂O₃ also helps to produce a clean toe line, which is especially beneficial in fillet welds [131]. The average austenitic stainless steel weld deposit typically contains 0.02 wt.-% bismuth (200 ppm). Bismuth can be added to the slag concept of flux-cored wires in more than one way and this is a recipe and formula secret of each individual flux-cored wire manufacturer. In the past, the bismuth content was not always analyzed nor reported. EN ISO 17633 [132] from 2017 only mentions that bismuth should be restricted to 20-ppm maximum for alloys intended

for high temperature. It became mandatory in AWS A5.22 [133] in 2012 to report the content if bismuth is intentionally added, or if it is known to be present at levels greater than 0.002%.

After several reports were published on intergranular cracking and premature creep failure in austenitic welds after a period of service at 650–750 °C [134–136], the use of bismuth as intentional alloying element has generally been limited to applications below 480 °C. The bismuth effect is essentially a solid-state reheat cracking or relaxation cracking mechanism. Nishimoto et al. [137] used Auger analysis to reveal the presence of bismuth on the fractured surface of austenitic stainless steels and drew the conclusion that segregation on the dendrite or grain boundaries was responsible for intergranular weld cracking at temperatures between 650 and 825 °C. Konosu et al. [138] carried out creep tests at 650 °C on type E308 FCAW weld metal with 230-ppm bismuth and concluded that flux-cored wires alloyed with bismuth caused segregation of bismuth in the grain boundaries and that this was harmful with respect to creep ductility and creep crack growth properties. Tsukimoto et al. [139] studied the effect of bismuth on reheat cracking susceptibility in E308H FCAW weld metal and it was suggested that bismuth segregation was responsible for reheat cracking at temperatures around 700 °C. API [140] has thus incorporated a limit of 20-ppm bismuth in austenitic stainless steel FCAW deposits, when these weld metals are exposed to temperatures above 1000°F (538 °C) during post-weld heat treatment (PWHT) or during service. AWS A5.22 [133] states that stainless steel electrodes containing bismuth additions should not be used for high-temperature service or PWHT above about 900°F (500 °C).

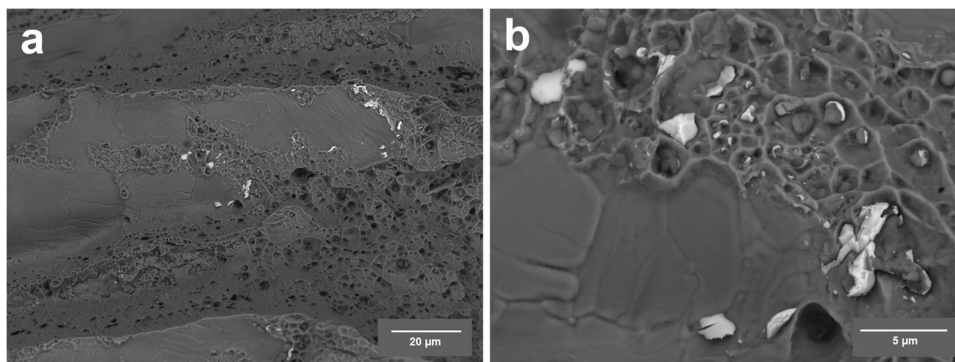
The maximum service temperature for duplex stainless steels is mostly set at 250 °C, and for this low temperature, no negative influence of bismuth on cracking sensitivity has been reported. It is, however, known that addition of bismuth oxide, Bi_2O_3 , has a measurable somewhat negative effect on the impact toughness in austenitics [139, 141]. Hara et al. [136] investigated the effect of small amounts of bismuth in the weld metal on the corrosion resistance and found no effect of bismuth remained in

the 308 type FCAW weld metal as compared to bismuth-free GTAW and SMAW weld metal. Ogawa et al. [142] have suggested that bismuth in duplex flux-cored wires has a negative impact on the corrosion resistance and thus revised the traditional pitting resistance equivalent formula to $\text{Cr} + 3.3 \times \text{Mo} + 16 \times \text{N} - 150 \times \text{Bi}$ for a PRE_{Bi} range of 33.0 to 43.0. The mechanism behind was not clarified, but the authors recommend that the use of bismuth should be limited to 0.015 wt.-%. Sugahara et al. [143] stated that preferably the use of Bi_2O_3 should be limited to 0.005 wt.-% in duplex stainless steel flux-cored wires, but no further information on the reasoning behind was given.

In the creep tests performed at 650 °C on type E308 FCAW weld metal with 230-ppm bismuth by Konosu et al. [138], there was no evidence of oxygen and it was concluded that bismuth exists as a single substance at the grain boundaries. This is of importance as the melting point for bismuth oxide Bi_2O_3 is 830 °C, while pure bismuth melts already at 270 °C [138]. Westin et al. [141] studied the risk for embrittlement of austenitic stainless steel flux-cored wires containing 180-ppm bismuth after PWHT at 700 °C and concluded that the decreased ductility is caused by bismuth segregating in grain boundaries with a particle-like distribution without any clear relation to oxygen.

Bismuth has been detected in hot cracks in duplex stainless steel weldments performed with the FCAW process [144, 145]. With scanning electron microscopy (SEM) in back-scatter mode, it is possible to visualize the element as a bright phase located in the flat region of the crack surface and in the surrounding dimples (Fig. 12). Bismuth is located attached to or as coating of MnS particles and is due to the low melting point and efficient wetting found deep in the last solidified metal of the cracks (Fig. 13). Bismuth has not been confirmed to make duplex weld metals susceptible — some flux-cored wires with elevated levels have been concluded to be resistant, while solidification cracks have also been found with bismuth-free wires [145]. It can, however, not be excluded that bismuth in combination with other elements such as, for instance, sulfur, phosphorous, and boron could contribute to crack formation [145].

Fig. 12 **a** Overview of the flat region of a solidification crack detected with a duplex flux-core wire of E2209T0 type and **b** surrounding dimples in higher magnification showing bismuth as a brighter phase and MnS as gray particles (fracture surface examined with SEM in back-scatter mode) [145]



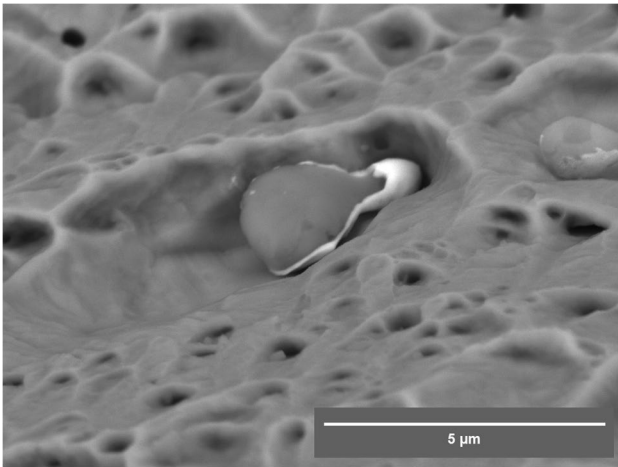


Fig. 13 MnS particle with partial coating of bismuth (fracture surface examined with SEM in back-scatter mode) [145]

7.6 Chemical composition and slag concept of flux-cored wires

The greater part of flux-cored wires consist of the sheath metal and the flux contributes elements for alloying, slag forming, and deoxidation. As compared to solid wires, the difference between various manufacturers is significant with different concepts and philosophies. Some set higher focus on slag removal, surface appearance, or mechanical properties, while others may optimize the wires to run on straight CO₂ or to lower the production costs to offer more customer-friendly prices. Although most suppliers get their raw materials from the same sources, the element content and size can be very different.

As the slag is detached after welding, a majority of the non-metallic flux constituents, but also a fraction of the weld metal impurities and alloying elements are removed as well. In contrast to solid wires, the welds performed with slag forming welding processes show more oxide inclusions and this generally has a negative effect on the impact toughness. Heat-to-heat variations may occur based on strip material heats, but also different lots of each and every raw material added to the flux. Although it is well known that sulfur and phosphorous are negative for the hot cracking resistance, these elements cannot be avoided in flux-cored wires due to some amounts in the strip material, but also as contamination of other raw materials. A certain amount of sulfur may in addition positively affect the weld bead penetration, fluidity of the weld metal, and possibly the slag detachability.

The behavior of a slag-covered process is challenging to predict. The driving forces (buoyancy, drag, arc pressure, electromagnetic, Marangoni pressure, and droplet impingement) and sulfur content are known to affect the molten pool flow and shape for GMAW [146]. The FCAW

process is further complicated by slag covering the droplets and the solidification temperature range for the slag cover. A wire with lower melting point or larger freezing range could thus be inherently more sensitive than an all-positional wire with rapid solidification [147]. The difference is also large between various wire producers with variations in intensity, arc stability, and slag concepts affecting the viscosity, interfacial tension, and conductivity. Different slags can have better desulfurizing activity [148] and prevent loss of alloying elements such as manganese and silicon [149]. A more rutile wire shows improved slag removal, while the impact toughness increases with a more basic wire. Zhang et al. [150] reported that the impact toughness in superduplex welds decreased when the pitting corrosion resistance increased. A flux-cored wire is consequently always a compromise.

8 Summary

Steel suppliers and wire manufacturers are aware of a few cases where solidification cracks have been found in welded duplex stainless steels, but it is unclear how much of this experience has been published. Although there are very few reports in the literature on hot cracking in duplex stainless steel weldments, it appears that all welding methods could under certain circumstances cause solidification cracking. The same elements known to form low-melting phases in austenitic stainless steel weldments are suggested to promote solidification cracking also in duplex alloys. The cracks are always located in the ferrite grain boundaries and low austenite contents may increase the susceptibility. The risk can, however, not be correlated to the phase balance only as cracks have been observed in welds with a wide range of ferrite. In the case of slag forming welding methods, the slag concept affecting the solidification range may influence the amount of low-melting phases being liquid at the critical strain rate at which cracks form. Some flux-cored wire formulations have been claimed to cause solidification cracking when welding thick-walled material, while other wires may successfully be used for the same application. It would thus be of interest to further evaluate duplex flux-cored wires on the susceptibility to hot cracking.

Acknowledgements Yngve Axelsson at Jernkontoret, Sweden, provided some of the older papers and reports. Prof. Carl E. Cross at Los Alamos National Laboratory is acknowledged for valuable comments on the script.

Declarations

Conflict of interest The author declares no competing interests.

References

- Ogawa T, Koseki T (1989) Effect of composition profiles on metallurgy and corrosion behavior of duplex stainless steel weld metals. *Weld J Res Suppl* 68(5):181s–191s. http://files.aws.org/wj/supplement/WJ_1989_05_s181.pdf. Accessed 28 Dec 2021
- Varol I, Baeslack WA III, Lippold JC (1992) Welding of duplex stainless steels. *Key Eng Mater* 69–70(1):217–251. <https://doi.org/10.4028/www.scientific.net/KEM.69-70.217>
- Gooch TG (1983) Weldability of duplex ferritic-austenitic stainless steels. *Proc. Duplex Stainless Steels '82*, St Louis, Mo, ASM, Metals Park, Ohio, Paper 8201–029:573–602
- Kou S (2003) *Welding metallurgy*. Second edition. John Wiley & Sons, Inc. ISBN: 0–471–43491–4. 480pp
- Kotecki DJ (1986) Ferrite control in duplex stainless steel weld metal. *Weld J Res Suppl* 65(10):273s–278s
- Liljas M, Qvarfort R (1986) Influence of nitrogen on weldments in UNS S31803. *Proc. Duplex Stainless Steels '86*, The Hague, NL, NIL, 244–256/acom 1–2:2–12
- Kudo T, Tsuge H, Moroishi T (1989) Stress corrosion cracking resistance of 22%Cr duplex stainless steel in simulated sour environments. *Corros* 45(10):831–838. <https://doi.org/10.5006/1.3584990>
- Liou H-Y, Hsieh R-I, Tsai W-T (2002) Microstructure and stress corrosion cracking in simulated heat-affected zones of duplex stainless steels. *Corros Sci* 44(12):2841–2856. [https://doi.org/10.1016/S0010-938X\(02\)00068-9](https://doi.org/10.1016/S0010-938X(02)00068-9)
- Omura T, Kushida T, Komizo Y (2000) Microstructural features and corrosion properties in laser welded duplex stainless steels. *Welding Int* 14(4):257–260. <https://doi.org/10.1080/09507110009549176>
- Pettersson R, Wessman S (2014) Critical analysis of the role of ferrite content in the environment-sensitive cracking of duplex stainless steels. *Proc. Eurocorr*, Pisa, Italy, Paper 7512:11pp. <http://eurocorr.efcw.org/2014/abstracts/4/7512.pdf>. Accessed 28 Dec 2021
- Shinozaki K, Ke L, North TH (1992) Hydrogen cracking in duplex stainless steel weld metal. *Weld J Res Suppl* 71(11):387s–396s
- Fredheim S, Mun CN (1992) Hydrogen induced cracking of duplex stainless steel weldments. *Proc. Offshore South East Asia*, Singapore, Paper OSEA92224:8pp.
- Pettersson RFA, Johansson E (2010) Stress corrosion resistance of duplex grades. *Proc. Duplex World 2010*, Beaune, France, KCI Publishing BV, The Netherlands, 12pp
- Jargelius-Pettersson RFA, Linder J, Hertzman S, Åström H (1993) Microstructure and stress corrosion cracking of duplex stainless steel welds, Report Number IM–2974, Swedish Institute for Metals Research
- Komenda J, Sandström R (1995) Quantitative characterisation of weld simulated structures in duplex stainless steel SAF 2205. *Acta Stereol* 14(1):29–34. <http://popups.uliege.be/0351-580x/index.php?id=663&file=1&pid=662> accessed on 2021–11–09
- Hoffmeister H, Lothongkum G (1994) Quantitative effects of nitrogen contents and cooling cycles on δ – γ transformation, chromium nitride precipitation and pitting corrosion after weld simulation of duplex stainless steels. *Proc. Duplex Stainless Steels '94*, Glasgow, Scotland, TWI, Paper 55, 2:12pp.
- Valiente Bermejo MA, Hurtig K, Eyzop D, Karlsson L (2019) A new approach to the study of multi-pass welds –microstructure and properties of welded 20-mm-thick superduplex stainless steel. *Appl Sci* 9(1050):18pp. <https://doi.org/10.3390/app9061050>
- Pickle T, Henry N, Morriss P, Tennis L, Wagner D, Baumer RE (2019) Root pass microstructure in super duplex stainless steel multipass welds. *Weld J* 98(5):123–134s. <https://doi.org/10.29391/2019.98.010>
- Hosseini VA, Hurtig K, Karlsson L (2020) Bead by bead study of a multipass shielded metal arc welded super duplex stainless steel. *Weld World* 64(2):283–299. <https://doi.org/10.1007/s40194-019-00829-7>
- Putz A, Althuber M, Zelić A, Westin EM, Willidal T, Enzinger N (2019) Methods for the measurement of ferrite content in multipass duplex stainless steel welds. *Weld World* 63(4):1075–1086. <https://doi.org/10.1007/s40194-019-00721-4>
- Varbai B, Adonyi Y, Baumer R, Pickle T, Dobránszky J, Májlinger K (2019) Weldability of duplex stainless steels – thermal cycle and nitrogen effects. *Weld J Res Suppl* 98(3):78s–87s. <https://doi.org/10.29391/2019.98.006>
- Ogura T, Matsumura T, Yu L, Kim DC, Inoue H, Oikawa Y, Saida K (2019) Numerical simulation of ferrite/austenite phase fraction in multipass welds of duplex stainless steels. *Proc. Mathematical Modelling of Weld Phenomena 12*, 12th International Seminar Numerical Analysis of Weldability, Graz, Austria, 31pp.
- Ramirez AJ, Lippold JC, Brandi SD (2003) The relationship between chromium nitride and secondary austenite precipitation in duplex stainless steels. *Metall Trans A* 34(8):1575–1597. <https://doi.org/10.1007/s11661-003-0304-9>
- Zhang Z, Jing H, Xu L, Han Y, Zhao L (2017) Influence of microstructure and elemental partitioning on pitting corrosion resistance of duplex stainless steel welding joints. *Corros Sci* 39(4):194–210. <https://doi.org/10.1016/j.apsusc.2016.10.047>
- Atamert S, King JE (1991) Elemental partitioning and microstructural development in duplex stainless steel weld metal. *Acta Metall Mater* 39(3):273–285. [https://doi.org/10.1016/0956-7151\(91\)90306-L](https://doi.org/10.1016/0956-7151(91)90306-L)
- Savage WF, Nippes EF, Erickson JS (1976) Solidification mechanisms in fusion welds. *Weld J Res Suppl* 55(8):213s–221s
- Savage WF, Lundin CD, Aronson AH (1965) Weld metal solidification mechanics. *Weld J Res Suppl* 44(4):175s–181s
- Bhatt RB, Kamat HS, Ghosal SK, De PK (1999) Influence of nitrogen in the shielding gas on corrosion resistance of duplex stainless steel welds. *J Mater Eng Perform* 8(5):591–597. <https://doi.org/10.1007/s11665-999-0014-6>
- Katayama S, Fujimoto T, Matsunawa A (1985) Correlation among solidification process, microstructure, microsegregation and solidification cracking susceptibility in stainless steel weld metals (Materials, Metallurgy & Weldability). *Transactions of JWRI* 14(1):123–138. <http://hdl.handle.net/11094/10942>. Accessed 28 Dec 2021
- Robinson JL, Scott MH (1980) Liquefaction cracking during the welding of austenitic stainless steels and nickel alloys. *Phil Trans R Soc Lond A* 295(1413):105–117. <https://doi.org/10.1098/rsta.1980.0079>
- Varol I, Baeslack WA III, Lippold JC (1989) Characterization of weld solidification cracking in a duplex stainless steel. *Metallurgy* 23(1):1–19. [https://doi.org/10.1016/0026-0800\(89\)90037-2](https://doi.org/10.1016/0026-0800(89)90037-2)
- Ogawa T, Koseki T (1987) Metallurgical investigation of weldments in nitrogen-enriched duplex stainless steel. *Proc. Welding and Performance of Pipelines 1986*, London, UK, 1:115–124
- Westin EM, Hertzman S (2014) Element distribution in lean duplex stainless steel welds. *Weld World* 58(3):143–160. <https://doi.org/10.1007/s40194-013-0108-5>
- Suutala N, Takalo T, Moisio T (1979) Austenitic solidification mode in austenitic stainless steel welds. *Metall Trans A* 10(8):1183–1190. <https://doi.org/10.1007/BF02811664>
- Thomas M, Vollert F, Weidemann J, Gibmeier J, Kromm A, Kannengießer T (2020) Surface- and volume-based investigation on influences of different Vrestraint testing parameters and chemical compositions on solidification cracking in LTT filler

- metals. *Weld World* 64(5):913–923. <https://doi.org/10.1007/s40194-020-00895-2>
36. Coniglio N, Cross CE (2020) Effect of weld travel speed on solidification cracking behavior. Part 1: Weld metal characteristics. *Int J Adv Manuf Technol* 107(11/12):5011–5023. <https://doi.org/10.1007/s00170-020-05231-y>
 37. Lippold JC, Kiser SD, DuPont JN (2011) *Welding metallurgy and weldability of nickel-base alloys*. John Wiley & Sons, Inc. 456pp. ISBN: 978–1–118–21003–1
 38. Lippold JC (2014) *Welding metallurgy and weldability*. John Wiley & Sons, Inc. 400pp. <https://doi.org/10.1002/9781118960332>
 39. Kou S (2015) A simple index for predicting the susceptibility to solidification cracking. *Weld J Res Suppl* 94(12):374s–388s
 40. Arata Y, Matsuda F, Saruwatari S (1974) Varestraint test for solidification crack susceptibility in weld metal of austenitic stainless steels. *Transactions of JWRI* 3(1):79–88. <http://hdl.handle.net/11094/3695>. Accessed 28 Dec 2021
 41. Nelson DE, Baeslack WA III, Lippold JC (1987) An investigation of weld hot cracking in duplex stainless steels. *Weld J Res Suppl* 66(8):241s–250s
 42. Prokhorov N (1962) The technological strength of metals while crystallizing during welding. *Weld Prod* 9(4):1–8
 43. Pumphrey WI, Lyons LV (1948) Cracking during the casting and welding of the more common binary aluminum alloys. *J Inst Met* 74:439–455
 44. Coniglio N, Cross CE (2009) Mechanisms for solidification crack initiation and growth in aluminum welding. *Metall Mater Trans A* 40(11):2718–2728. <https://doi.org/10.1007/s11661-009-9964-4>
 45. Rappaz M, Drezet J, Gremaud M (1999) A new hot-tearing criterion. *Metall Mater Trans A* 30(2):449–455. <https://doi.org/10.1007/s11661-999-0334-z>
 46. Brooks JA, Lambert FJ Jr (1978) The effects of phosphorous, sulfur and ferrite content on weld cracking of type 309 stainless steel. *Weld J Res Suppl* 57(5):139s–143s
 47. Lippold JC, Kotecki DJ (2005) *Welding metallurgy and weldability of stainless steels*. John Wiley & Sons, Inc., New Jersey. 376pp. ISBN: 978–0–471–47379–4
 48. Shankar VG, Gill TPS, Mannan SL, Sundaresan S (2003) Solidification cracking in austenitic stainless steel welds. *Sadhana* 28(3–4):359–382
 49. Kujanpää V, Suutala N, Takalo T, Moisio T (1979) Correlation between solidification cracking and microstructure in austenitic and austenitic-ferritic stainless steel. *Weld Res Int* 9(2):55–76
 50. Borland JCG, Younger RN (1960) Some aspects of cracking in welded Cr-Ni austenitic steels. *Br Weld J* 7:22–59
 51. Borland JCG (1960) Hot cracking in welds. *Br Weld J* 7:558–559
 52. Matsuda F, Nakagawa H, Uehara T, Katayama S, Arata Y (1979) A new explanation for role of delta-ferrite improving weld solidification cracks susceptibility in austenitic stainless steel. *Transactions of JWRI* 8(1):105–112. <http://hdl.handle.net/11094/5579>. Accessed 28 Dec 2021
 53. Yu PF, Thompson KJ, McCarthy J, Kou S (2018) Microstructure evolution and solidification cracking in austenitic stainless steel welds. *Weld J Res Suppl* 97(9):301s–314s
 54. Hull FC (1967) Effects of delta ferrite on the hot cracking of stainless steel. *Weld J Res Suppl* 46(9):399s–409s
 55. Takalo T, Suutala N, Moisio T (1979) Austenitic solidification mode in austenitic stainless steel welds. *Metall Trans* 10(8):1173–1181. <https://doi.org/10.1007/BF02811663>
 56. Liljas M (1995) The welding metallurgy of duplex stainless steels. *Proc. Duplex Stainless Steels '94*, Glasgow, Scotland, Vol. 2:Paper KV:15pp.
 57. Kujanpää V, Suutala N, Takalo T, Moisio T (1980) Solidification cracking – estimation of the susceptibility of austenitic and austenitic-ferritic stainless steel welds. *Metal Constr* 12(6):282–285
 58. Kujanpää V (1985) Effect of steel type and impurities in solidification cracking of stainless steel welds. *Metal Constr* 17(1):40R–46R
 59. Matsuda F, Nakagawa H, Kato I, Murata Y (1986) Solidification crack susceptibility in weld metals of duplex stainless steels. *Transactions of JWRI* 15(1):99–112. <http://hdl.handle.net/11094/10729>. Accessed 28 Dec 2021
 60. Tynell M (1983) Applicability range for a high-strength duplex stainless steel in deep sour oil and gas wells. *Proc. Duplex Stainless Steels '82*, ASM, Metals Park, Ohio, 282–292
 61. Miyki H, Kudo T, Kuso M, Miura M, Moroishi T (1983) 25%Cr containing duplex phase stainless steel for hot sea water application. *Proc. Duplex Stainless Steels '82*, ASM, Metals Park, Ohio, 95–112
 62. Cieslak MJ, Ritter M, Savage F (1982) Solidification cracking and analytical electron microscopy of austenitic stainless steel weld metal. *Weld J Res Suppl* 61(1):1s–8s
 63. Cross CE, Böllinghaus T (2016) The effect on restraint on weld solidification cracking in aluminum. *Weld World* 50(11/12):51–54. <https://doi.org/10.1007/BF03263461>
 64. Coniglio N, Cross CE (2013) Initiation and growth mechanism for weld solidification cracking. *Int Mat Rev* 58(7):375–397. <https://doi.org/10.1179/1743280413Y.0000000020>
 65. Kannengiesser T, Boellinghaus T (2014) Hot cracking tests – an overview of present technologies and applications. *Weld World* 58(5):397–421. <https://doi.org/10.1007/s40194-014-0126-y>
 66. ASME IX (2019) *ASME Boiler and Pressure Vessel Code, Section IX: Welding and Brazing Qualifications*. American Society of Mechanical Engineering. 422pp. ISBN 9780791872901
 67. Honeycombe J, Gooch TG (1973) Effects of microcracks on mechanical properties of austenitic stainless-steel weld- metals. *Br Weld J* 5(4):140–147
 68. Yeniscavich W (1966) The effect of fissures on the fatigue strength of Ni-Cr-Fe alloys. *Weld J Res Suppl* 45(3):111s–123s
 69. Vishnu R, Brorson A, Holmberg B (1999) Microfissures in super-austenitic stainless steel weldments and their effect on fatigue properties. *Proc. Stainless Steel World*, KCI Publ. BV, Zutphen, The Netherlands, Paper SSW99–056:131–140
 70. Ogawa T, Tsunetomi E (1982) Hot cracking susceptibility of austenitic stainless steels. *Weld J Res Suppl* 61(3):82s–93s
 71. Arata Y, Matsuda F, Katayama S (1976) Solidification crack susceptibility in weld metals of fully austenitic stainless steels (Report I): Fundamental investigation on solidification behavior of fully austenitic and duplex microstructures and effect of ferrite on microsegregation. *Transactions of JWRI* 5(2):35–51. <http://hdl.handle.net/11094/7813>. Accessed 28 Dec 2021
 72. Arata Y, Matsuda F, Katayama S (1977) Solidification crack susceptibility in weld metals of fully austenitic stainless steels (Report II): effect of ferrite, P, S, C, Si and Mn on ductility properties of solidification brittleness. *Transactions of JWRI* 6(1):105–116. <http://hdl.handle.net/11094/8229>. Accessed 28 Dec 2021
 73. Arata Y, Matsuda F, Nakagawa H, Katayama S, Ogata S (1977) Solidification crack susceptibility in weld metals of fully austenitic stainless steels (Report III): effect of strain rate on cracking threshold in weld metal during solidification. *Transactions of JWRI* 6(2):37–46. <http://hdl.handle.net/11094/9667>. Accessed 28 Dec 2021
 74. Arata Y, Matsuda F, Nakagawa H, Katayama S (1978) Solidification crack susceptibility in weld metals of fully austenitic stainless steels (Report IV): effect of decreasing P and S on solidification crack susceptibility of SUS 310S austenitic stainless steel weld metals. *Transactions of JWRI* 7(2):21–24. <http://hdl.handle.net/11094/6740>. Accessed 28 Dec 2021

75. Matsuda F, Katayama S, Arata Y (1981) Solidification crack susceptibility in weld metals of fully austenitic stainless steels (Report V): solidification crack susceptibility and amount of phosphide and sulphide in SUS 310S weld metals. *Transactions of JWRI* 10(2):73–84. <http://hdl.handle.net/11094/11708>. Accessed 28 Dec 2021
76. Matsuda F, Nakagawa H, Katayama S, Arata Y (1982) Solidification crack susceptibility in weld metals of fully austenitic stainless steels (Report VI): effect of La or REM addition on solidification crack resistance. *Transactions of JWRI* 11(1):79–94. <http://hdl.handle.net/11094/6079>. Accessed 28 Dec 2021
77. Matsuda F, Nakagawa H, Katayama S, Arata Y (1982) Solidification crack susceptibility in weld metals of fully austenitic stainless steels (Report VII): effect of Mn and N on solidification crack resistance. *Transactions of JWRI* 11(2):79–85. <http://hdl.handle.net/11094/7004>. Accessed 28 Dec 2021
78. Matsuda F, Nakagawa H, Katayama S, Arata Y (1983) Solidification crack susceptibility in weld metals of fully austenitic stainless steels (Report VIII): effect of nitrogen on cracking in SUS 304 weld metals (materials, metallurgy & weldability). *Transactions of JWRI* 12(1):89–95. <http://hdl.handle.net/11094/10593>. Accessed 28 Dec 2021
79. Matsuda F, Katayama S, Arata Y (1983) Solidification crack susceptibility in weld metals of fully austenitic stainless steels (Report IX): effect of titanium on solidification crack resistance (materials, metallurgy & weldability). *Transactions of JWRI* 12(2):247–252. <http://hdl.handle.net/11094/11967>. Accessed 28 Dec 2021
80. Yamada K, Hamada M, Motoya D, Nakatsuka S, Amaya H, Takabe H (2013) Process for producing welded joint. European Patent Specification EP 2 832 487 B1. 24pp.
81. Gong W, Wang P, Zhang L, Jiang Z (2020) Effects of Ce on microstructure and mechanical properties of LDX 2101 duplex stainless steel. *Metals* 10(1233):12. <https://doi.org/10.3390/met10091233>
82. Myllykoski L, Suutala N (1983) Effect of solidification mode on hot ductility of austenitic stainless steels. *Met Technol* 10(1):453–460. <https://doi.org/10.1179/030716983803291307>
83. Melford DA (1980) The influence of residual and trace elements on hot shortness and high temperature embrittlement. *Phil Trans R Soc Lond A* 295(1413):89–101
84. Tehovnik F, Vodopivec F, Celin R, Arzenš B, Gontarev B (2011) Effect of δ -ferrite, lead and sulphur on hot workability of austenitic stainless steels with solidification structure. *Mater Sci Technol* 2(4):774–782. <https://doi.org/10.1179/026708311X12916291424272>
85. Walsh JM, Anderson NP (1976) Characterization of nickel-base superalloy fracture surfaces by Auger electron spectroscopy. *Proc. Superalloys Seven Springs Conference, AIME/TMS*:127–136
86. Bergh S (1949) Influence of lead on behavior of stainless steel. *Iron Age* 164(14/7):96–99; *Met Rev* 22(9):32
87. Jensfeld PM, Norrman TO (1962) Bismuth and its effect on hot workability of stainless steel. *Jernkontor Annlr* 146(6):438–452
88. Cole AT, Richardson GJ (1980) Hot Working and forming processes. The Metals Society, London, pp 128–132
89. Ljungström LG (1977) Influence of trace elements on the hot ductility of austenitic 17Cr13NiMo-steel. *Scand J Metall* 6:176–184
90. Norström L-Å (1979) A comment on the influence of trace elements on the hot ductility of austenitic 17Cr 13Ni Mo-steel. *Scand J Metall* 8(2):95–96
91. Skoglund E (1979) Inverkan av föroreningar på rostfria ståls varmbearbetbarhet. Jernkontorets forskningsuppgift, Internal report JK 493/73 (in Swedish)
92. Castro R, de Cadenet JJ (1974) *Welding metallurgy of stainless and heat-resisting steels*, Cambridge University Press, Cambridge. ISBN: 9780521204316
93. Blumfield D, Clark GA, Guha P (1981) Welding duplex austenitic-ferritic stainless steel weldments. *Metal Constr* 13(5):269–273
94. Flasche LH (1983) Weldability of Ferralium alloy 255. *Proc. Duplex Stainless Steels '82*, ASM, Metals Park, Ohio, 553–572
95. Honeycombe J, Gooch TG (1977) Intergranular attack in welded stress-corrosion resistant stainless steel. *Weld J Res Suppl* 56(11):339s–353s
96. Karlsson L (2012) Welding duplex stainless steels – a review of current recommendations. *Weld World* 56(3):65–76. <https://doi.org/10.1007/BF0321351>
97. Fellman A, Westin EM (2008) Fiber laser hybrid welding of stainless steels. *Proc. ICALEO® Congress Materials Processing Conference, Temecula, CA*. Paper #1204:545–553
98. Cross CE, Coniglio N, Westin EM, Gumenyuk A (2011) Laser weldability of stainless steel. Hot cracking phenomena in welds III, Springer-Verlag Berlin and Heidelberg GmbH & Co. K, Berlin, Germany, 131–144. ISBN: 9783642168635
99. Jadav HH, Sharma DG, Nanavati PK, Vyas H, Menghani JM (2015) Studies on hot cracking susceptibility of duplex stainless steel. NCEETM Indus University. 4pp.
100. Saida K, Ogura T (2018) Hot cracking susceptibility in duplex stainless steel welds. *Mater Sci Forum* 941:679–685. <https://doi.org/10.4028/www.scientific.net/MSF.941.679>
101. Hoberg B (2021) Private communication
102. Westin EM, Westerberg LG, Grain growth and austenite reformation in duplex stainless steel heat-affected zones. Part 1 – Comparison of Gleeble® simulations with actual welds in UNS S32101, ongoing work in preparation for Welding in the World
103. Torkhov GF, Slyshankova VA, Ul'yanin EA, Sherevera AV (1978) Structure and properties of high-nitrogen corrosion-resistant austenitic steels. *Met Sci Heat Treat* 20(11):887–890. <https://doi.org/10.1007/BF00713747>
104. Rashec TV, Dzhabazova LP, Kovachevaa RS, Andreev CA (1981) Processes of precipitation and intercrystalline corrosion in high-nitrogen Cr-Mn steels after isothermal annealing. *Met Sci Heat Treat* 23(5):310–313. <https://doi.org/10.1007/BF00700539>
105. Vanderschaeve F, Taillard R, Focq J (1995) Discontinuous precipitation of Cr₂N in a high-nitrogen chromium-manganese austenitic stainless steel. *J Mat Sci* 30(12):6035–6046. <https://doi.org/10.1007/BF01151525>
106. Prohaska M (2012) Private communication
107. Coniglio N, Cross CE (2020) Effect of weld travel speed on solidification cracking behavior. Part 2: Testing conditions and metrics. *Int J Adv Manuf Technol* 107(11/12):5025–5038. <https://doi.org/10.1007/s00170-020-05232-x>
108. Coniglio N, Cross CE (2020) Effect of weld travel speed on solidification cracking behavior. Part 3: Modeling. *Int J Adv Manuf Technol* 107(4):5039–5051. <https://doi.org/10.1007/s00170-020-05233-w>
109. Savage WF, Aronson AH (1966) Preferred orientation in the weld fusion zone. *Weld J Res Suppl* 45(2):85s–89s
110. Davies GJ, Garland JG (1975) Solidification structures and properties of fusion welds. *Int Metall Rev* 20:83–108
111. Morgan-Warren EJ, Jordan MF (1976) Effect of travel speed on solidification cracking in autogenous tungsten inert gas arc welding of low-alloy steel sheet. *Met Technol* 3(1):29–40. <https://doi.org/10.1179/030716976803391421>
112. Chen WF (1997) *Handbook of structural engineering*, CRC Press LCC, Boca Raton, New York, 1600pp. ISBN 0–8493–2674–5
113. Norman B (1994) *Weldability of ferritic steels*. Abington Publishing, Cambridge, UK. 300pp. ISBN 1 85573 092 8
114. Westin EM. Modified FISCO test for ranking the solidification cracking susceptibility of duplex flux-cored wires. Ongoing work planned to be published in *Welding in the World*
115. EN ISO 15156–3 (2020) *Petroleum and natural gas industries – materials for use in H₂S-containing environments in oil and gas protection. Part 3: Cracking-resistant CRAs (corrosion resistant alloys) and other alloys*. European Committee for Standardization, Brussels, Belgium. 80pp.

116. Gunn RN (1997) Duplex stainless steels: microstructure, properties and applications. Woodhead Publishing Ltd, Cambridge ISBN 9781855733183
117. Karlsson L (2000) Welding of stainless steels. Duplex and superduplex steels. *Weld Int* 14:5–11. <https://doi.org/10.1080/09507110009549131>
118. Berglund G, Wilhelmsson P (1989) Fabrication and practical experience of duplex stainless steels. *Mater Des* 10:23–28
119. Knyazeva MF, Pohl M (2013) Duplex steels: part I: genesis, formation, structure. *Metallogr Microstruct Anal* 2:113–121. <https://doi.org/10.1007/s13632-013-0066-8>
120. Liljas M, Gemmel G (2000) Choice of specifications and design codes for duplex stainless steels. *Proc. Duplex America 2000*, Houston, TX, Paper DA2–031:199–209
121. ISO 17781 (2017) Petroleum, petrochemical and natural gas industries – test methods for quality control of microstructure of ferritic/austenitic (duplex) stainless steels. ISO copyright office, Geneva, Switzerland. 34pp.
122. Carpenter KR, Monaghan BJ, Norrish J (2009) Analysis of fume formation rate and fume particle composition for gas metal arc welding (GMAW) of plain carbon steel using different shielding gas compositions. *ISIJ Int* 49(3):416–420. <https://doi.org/10.2355/isijinternational.49.416>
123. Kah P, Martikainen J (2013) Influence of shielding gases in the welding of metals. *Int J Adv Manuf Technol* 64:1411–1421. <https://doi.org/10.1007/s00170-012-4111-6>
124. Morozova J, Bonnel J-M, Rosert R, Ossenbrink R, Michailov V (2019) Influence of the welding position during flux cored arc welding on impact toughness of stainless and low alloy steel weld metals. *DVS Berichte Band 355*:310–318 (in German). ISBN 978–3–96144–066–5
125. Li T, Zhang Y, Gao L, Zhang Y (2018) Optimization of FCAW parameters for ferrite content in 2205 DSS welds based on the Taguchi design method. *Adv Mater Sci Eng* 7950607:7. <https://doi.org/10.1155/2018/7950607>
126. Palandi M, Magudeeswaran G, Harikannan N (2019) Optimization of pulsed current flux cored arc welding parameters for ferrite phase in duplex stainless steel welds. *J Balk Tribol Assoc* 25(4):865–881
127. Kou S (2003) Solidification and liquation cracking issues in welding. *JOM* 55(6):37–42. <https://doi.org/10.1007/s11837-003-0137-4>
128. Sterjovski Z, Bayley C, Donato J, Lane N, Lang D (2014) Weld-end solidification cracking in pulsed tandem gas metal arc welding of naval steels. *Weld J Res Suppl* 93(5):145s–152s
129. Godai T, Minato S, Nishimura K, Ogawa T (1982) Composite wire for stainless steel welding. U.S. Patent 4,345,140. 7pp. <https://patentimages.storage.googleapis.com/15/c3/cc/0747e7958c52be/US4345140.pdf>. Accessed 28 Dec 2021
130. Mizukami H, Nagakura Y, Kusakawa K (1989) Effect of surface active element on the initial solidification structure of stainless steel ingot. *ISIJ Int* 75(8):1308–1315
131. Farrar JCM, Marshall AW, Zhang Z (2001) Position statement on the effect of bismuth on the elevated temperature properties of flux cored stainless steel weldments. *Weld World* 45(5/6):25–31
132. EN ISO 17633 Welding consumables – Tubular cored electrodes and rods for gas shielded and non-gas shielded metal arc welding of stainless and heat-resisting steels – Classification (2018) European Committee for Standardization, Brussels, Belgium. 46pp
133. AWS A5.22/A5.22M:2012 Specification for stainless steel flux cored and metal cored welding electrodes and rods, Fourth Edition, American Welding Society, Miami, FL, 68pp
134. Chemical Plant Welding Research Committee of the Japan Engineering Society (JWES) (1996) High temperature damage to stainless steel welds made by flux-cored arc welding and its analysis. *Proc. API 61th Fall Refinery Meeting*, pp. 21–23
135. Nishiyama S, Matushita Y, Maruyama T (1995) Flux-cored wires for stainless steel welding. *Weld World* 36(6):103–123. Pergamon Press. ISSN: 0043–2288
136. Hara Y, Shiga K, Nakazawa N (1996) High temperature damage to stainless steel welds made by flux cored arc welding and its analysis. *Proc. API 61st Full Refinery Meeting*, Houston, TX
137. Nishimoto K, Matsunaga T, Tanaka T, Okazaki T (1998) Effect of bismuth on reheat cracking susceptibility in type 308 FCAW weld metal. *Weld World* 41(3):220–235. Pergamon Press. ISSN: 0043–2288
138. Konosu S, Hashimoto A, Mashiba H, Takeshima T, Ohtsuka T (1998) Creep crack growth properties of type 308 austenitic stainless steel weld metals. *Weld J Res Suppl* 77(8):22s–327s
139. Tsukimoto K, Toyoda M, Matsumoto O, Kawaguchi S (1998) Effect of elements on weldability and hot ductility of FCAW stainless steel weld metal. *Weld World* 41(3):240–252. Pergamon Press. ISSN: 0043–2288
140. API RP 582 (2009) Welding guidelines for the chemical, oil, and gas industries, 2nd Edition, American Petroleum Institute, Washington DC, 14pp
141. Westin EM, Schnitzer R, Ciccomascolo F, Maderthoner A, Grönlund K, Runnsjö G (2016) Austenitic stainless steel bismuth-free flux-cored wires for high-temperature applications. *Weld World* 60(6):1147–1158. <https://doi.org/10.1007/s40194-016-0376-y>
142. Ogawa T, Maruyama T, Ozaki S (2002) Flux cored wire for welding duplex stainless steel. United States Patent US 6,340,396 B1. 12pp
143. Sugahara H, Ikeda T, Watanabe H (2010) Flux-cored wire for stainless steel arc welding. United States Patent Application Publication US 2011/0139761 A1. 9pp
144. Westin EM, Putz A, Maderthoner A, Pilhagen J (2022) Solidification cracking in duplex stainless steel flux-cored arc welds Part 1 – Cracking in 30 mm thick material welded under high restraint. In preparation for *Welding in the World*
145. Westin EM, Warchomicka F (2022) Solidification cracking in flux-cored welding of duplex stainless steel Part 2 – Cracking in 22Cr all-weld metal under high restraint. In preparation for *Welding in the World*
146. Cho W-I, Na S-J (2021) Impact of driving forces on molten pool in gas metal arc welding. *Weld World* 65(9):1735–1747. <https://doi.org/10.1007/s40194-021-01138-8>
147. Holly S, Mayr P, Bernhard C, Posch G (2018) Slag characterization of 308L-type stainless steel flux-cored wires. *Weld World* 63(2):293–311. <https://doi.org/10.1007/s40194-018-0675-6>
148. Brown SD, Roxburgh RJ, Ghita I, Bell HB (1982) Sulphide capacity of titania-containing slags. *Ironmaking Steelmaking* 9(4):163–167
149. Iwamoto N (1983) Structure of slag (XI) – role of TiO₂ in slag. *Transactions of JWRI* 12(1):131–141. <http://hdl.handle.net/11094/8829>. Accessed 28 Dec 2021
150. Zhang Z, Golding M, van der Mee V (2018) Pitting corrosion resistance properties of super duplex stainless steel weld metals and influencing factors. *Weld World* 63(3):663–672. <https://doi.org/10.1007/s40194-018-00684-y>

Publisher's Note Springer Nature remains neutral with regard to jurisdictional claims in published maps and institutional affiliations.